

**Unified theory of consequences of spontaneous emission in a  $\Lambda$  system**Sophia E. Economou,<sup>1</sup> Ren-Bao Liu,<sup>1</sup> L. J. Sham,<sup>1</sup> and D. G. Steel<sup>2</sup><sup>1</sup>*Department of Physics, University of California San Diego, La Jolla, California 92093-0319, USA*<sup>2</sup>*The H. M. Randall Laboratory of Physics, University of Michigan, Ann Arbor, Michigan 48109, USA*

(Received 19 January 2005; published 26 May 2005)

In a  $\Lambda$  system with two nearly degenerate ground states and one excited state in an atom or quantum dot, spontaneous radiative decay can lead to a range of phenomena, including electron-photon entanglement, spontaneously generated coherence, and two-pathway decay. We show that a treatment of the radiative decay as a quantum evolution of a single physical system composed of a three-level electron subsystem and photons leads to a range of consequences depending on the electron-photon interaction and the measurement. Different treatments of the emitted photon channel the electron-photon system into a variety of final states. The theory is not restricted to the three-level system.

DOI: 10.1103/PhysRevB.71.195327

PACS number(s): 78.67.Hc, 42.50.Md, 42.50.Ct

**I. INTRODUCTION**

The electromagnetic vacuum is commonly considered as a reservoir which causes decoherence and decay of a quantum mechanical system coupled to it. An alternative view holds that the two subparts (“quantum system” and “bath”) are constituents of a single closed quantum mechanical whole, which is governed by unitary evolution until a projection (measurement) is performed. Different projections may give rise to a variety of phenomena which on the surface appear unrelated. Spontaneous emission is a quantum phenomenon which has been treated in both ways. Its effects are of interest from the views of both fundamental physics and applications.

The radiative decay of a three-level system is attractive for its simplicity and yet richness in physical phenomena. A variety of effects follow from the spontaneous decay. Those which involve semiclassical light and ensemble of atoms include the electromagnetically induced transparency<sup>1</sup> and lasing without inversion.<sup>2</sup> By definition, a  $\Lambda$  system has two nearly degenerate ground states which are dipole coupled to one excited state for optical transitions. We shall, for conciseness, refer to the states as electronic states in an atom or quantum dot. The decoherence and decay effects for a single  $\Lambda$  system are relevant to quantum computing and information processing, for example, in many implementation schemes,<sup>3–7</sup> which can be more practical than the direct excitation of the two-level system.

A  $\Lambda$  system initially in the excited state will eventually decay by the emission of a photon. This process may result in the entanglement of the  $\Lambda$  system with the emitted photon. Recently, entanglement between the hyperfine levels of a trapped ion and the polarization of a photon spontaneously emitted from the ion was demonstrated experimentally.<sup>8</sup>

In quantum optics of the atom, coupling to the modes of the electromagnetic vacuum can contribute to coherence between atomic states, and such terms have been implicit in the textbook treatment of spontaneous radiative decay<sup>9</sup> or indeed explicit in research papers.<sup>10</sup> In the early 1990s, it was pointed out that in a  $\Lambda$  system the spontaneous decay of the highest state to the two lower ones may result in a coherent superposition of the two lower states.<sup>11</sup> The conditions for

this spontaneously generated coherence (SGC) as presented in Ref. 11 are that the dipole matrix elements of the two transitions are nonorthogonal and that the difference between the two frequencies is small compared to the radiative linewidth of the excited state.

The final example is the so-called two-pathway decay in which a  $\Lambda$  system—as opposed to a  $V$  system—cannot exhibit quantum beats because the information on which the decay path of the system is in principle available by detection of the atom, and therefore no beats are expected (p. 19 of Ref. 12).

All of the phenomena listed above, when viewed separately, appear unrelated, if not down-right contradictory. In fact, they stem from the same process, namely the radiative spontaneous decay of a  $\Lambda$  system. The primary purpose of this paper is to show how they naturally emerge from the same time-evolved composite state of the whole system ( $\Lambda$  subsystem and the electromagnetic modes). From this treatment, follow the conditions for each effect in terms of the electron-photon coupling and in terms of different ways of projecting the photon state by measurement. We also show how a change of symmetry of the system—by the introduction of a perturbation—may determine whether or not a SGC will occur.

The second goal of this work is to analyze these effects in the solid state, where the two lower levels of the  $\Lambda$  system are the spin states of an electron confined in a semiconductor quantum dot. For this system, SGC has been given a theoretical analysis and experimental demonstration,<sup>13</sup> and we further propose here an experiment for the demonstration of spin-photon polarization entanglement. In our treatment, we distinguish between a single system and an ensemble for the various phenomena; in this context, we make a comparative study of the solid-state and the atomic system.

This paper is organized as follows. In Sec. II, we present the time evolution of the decay process which leads to the conditions for the occurrence of each of the listed phenomena. In Sec. III, we deduce a set of conditions on the symmetry of the system for SGC. Sections IV and V illustrate these conditions by specific examples from atomic and solid-state systems, respectively. We also present the theory of the

pump-probe experiment and derive the probe signal, which is altered by the SGC term (Sec. VI).

## II. SPONTANEOUS EMISSION AS QUANTUM EVOLUTION

Consider a single  $\Lambda$  system in a photon bath with modes  $|k\rangle$ , where  $k=(\mathbf{k}, \sigma)$ ,  $\mathbf{k}$  being the wave vector and  $\sigma$  the state with the polarization vector  $\boldsymbol{\epsilon}_\sigma$ . In the dipole and rotating-wave approximation, the Hamiltonian for the whole system is given by

$$H = \sum_k \omega_k b_k^\dagger b_k + \sum_{i=1}^3 \epsilon_i |i\rangle\langle i| + \sum_{k:i=1,2} g_{ik} b_k^\dagger |i\rangle\langle 3| + \sum_{k:i=1,2} g_{ik}^* b_k |3\rangle\langle i|, \quad (1)$$

where  $b_k$  destroys a photon of energy or frequency  $\omega_k$  ( $\hbar=1$ ) and  $|i\rangle$  is the electronic state with energy or frequency  $\epsilon_i$ . The coupling between the photon and the electron is  $g_{ik} \propto \boldsymbol{\epsilon}_\sigma \cdot \mathbf{d}_i$ , where  $\mathbf{d}_i$  is the dipole matrix element for the transition  $3 \leftrightarrow i$ . The  $\Lambda$  system is taken to be at  $t=0$  in the excited level  $|3\rangle$  (which can be prepared by a short pulse), and the photon bath is in the vacuum state, i.e., the whole system is in a product state. For  $t>0$ , the composite wave packet can be written as

$$|\psi(t)\rangle \equiv c_3(t)|3\rangle|\text{vac}\rangle + \sum_k c_{1k}(t)|1\rangle|k\rangle + \sum_k c_{2k}(t)|2\rangle|k\rangle, \quad (2)$$

where  $|\text{vac}\rangle$  is the photon vacuum state. Evolution of this state is governed by the Schrödinger equation.

By the Weisskopf–Wigner theory<sup>14</sup> of spontaneous emission,<sup>12</sup> the coefficient  $c_3$  is obtained by one iteration of the other coefficients:

$$\begin{aligned} \partial_t c_3 = & -i\epsilon_3 c_3 - \sum_k |g_{1k}|^2 \int_0^t e^{-i(\epsilon_1 + \omega_k)(t-t')} c_3(t') dt', \\ & - \sum_k |g_{2k}|^2 \int_0^t e^{-i(\epsilon_2 + \omega_k)(t-t')} c_3(t') dt'. \end{aligned} \quad (3)$$

Since the electron–photon coupling is much weaker than the transition energy in the  $\Lambda$  system, the integrals in the equation above can be evaluated in the Markovian approximation, resulting in:

$$\partial_t c_3 \approx -i\epsilon_3 c_3 - \frac{\Gamma_{31}}{2} c_3 - \frac{\Gamma_{32}}{2} c_3, \quad (4)$$

where

$$\Gamma_{3i} = 2 \sum_k |g_{2k}|^2 \int_0^t e^{-i(\epsilon_i + \omega_k)(t-t')} dt'. \quad (5)$$

Thus, the solution is

$$c_3 \approx e^{-i(\epsilon_3 + \Gamma/2)t}, \quad (6)$$

where  $\Gamma \equiv \Gamma_{31} + \Gamma_{32}$  is the radiative linewidth of the excited state. Furthermore,  $c_{1k}$  and  $c_{2k}$  are given by

$$c_{1k} \approx - \frac{g_{1k}}{\epsilon_3 - \epsilon_1 - \omega_k - i\frac{\Gamma}{2}} \left[ e^{-i(\epsilon_1 + \omega_k)t} - e^{-i\epsilon_3 t - \frac{\Gamma}{2}t} \right],$$

$$c_{2k} \approx - \frac{g_{2k}}{\epsilon_3 - \epsilon_2 - \omega_k - i\frac{\Gamma}{2}} \left[ e^{-i(\epsilon_2 + \omega_k)t} - e^{-i\epsilon_3 t - \frac{\Gamma}{2}t} \right].$$

In order to study the system in the  $2 \times 2$  subspace of the lower states, we take the limit  $t \gg \Gamma^{-1}$ . After the spontaneous emission process, the final state is a electron–photon wave-packet  $\sum_{k:i=1,2} c_{ik} |i\rangle|k\rangle$ , with the coefficients

$$c_{1k} \approx - \frac{g_{1k}}{\epsilon_3 - \epsilon_1 - \omega_k - i\frac{\Gamma}{2}} e^{-i(\epsilon_1 + \omega_k)t}, \quad (7)$$

$$c_{2k} \approx - \frac{g_{2k}}{\epsilon_3 - \epsilon_2 - \omega_k - i\frac{\Gamma}{2}} e^{-i(\epsilon_2 + \omega_k)t}. \quad (8)$$

The state of a photon is specified by its propagation direction  $\mathbf{n}$ , polarization  $\sigma(\boldsymbol{\epsilon}_\sigma \perp \mathbf{n})$ , and frequency  $\omega$ . So, we can formulate the total wave packet as

$$\sum_{\mathbf{n}, \sigma} [g_{1\sigma} e^{-i\epsilon_1 t} |1\rangle|\mathbf{n}, \sigma, f_1(t)\rangle + g_{2\sigma} e^{-i\epsilon_2 t} |2\rangle|\mathbf{n}, \sigma, f_2(t)\rangle], \quad (9)$$

where we have taken the coupling constants to be frequency-independent. In Eq. (9)  $f_j(t)$  is the pulse shape of the photon. From Eqs. (7) and (8), we see that the photon wave packet has a finite bandwidth; this point, which was first studied by Weisskopf and Wigner in their classic treatment of spontaneous emission,<sup>14</sup> is reflected in the structure of  $f_j(t)$ . These functions have a central frequency equal to  $\epsilon_3 - \epsilon_j$  and a bandwidth equal to  $\Gamma$ . As a consequence of the finite bandwidth, for a given propagation direction and polarization, the basis states  $\{|\mathbf{n}, \sigma, f_j\rangle\}$  are not orthogonal, the overlap between them being

$$\langle \mathbf{n}, \sigma, f_i | \mathbf{n}, \sigma, f_j \rangle = \frac{i\Gamma}{i\Gamma + \epsilon_{ij}}, \quad (10)$$

where  $\epsilon_{ij} = \epsilon_i - \epsilon_j$ .

We should emphasize that the wave packet formed in Eq. (9) does not rely on the Markovian approximation. In a full quantum kinetic description of the photon emission process, the wave packet of the whole system would still have the same form, the central frequency and bandwidth of the pulses would be close to those found using the Markovian approximation, but the specific profile of  $f_j(t)$  would be different from those given by Eqs. (7) and (8).

The various phenomena (electron and photon polarization entanglement, SGC, and two-pathway decay) can all be derived from the wave packet of Eq. (9).

If the spontaneously emitted photon is not detected at all, we have to average over the ensemble of photons of all possible propagation directions to obtain the electronic state. This is the usual textbook treatment of spontaneous emis-

sion. However, if detection of an emitted photon leads to a knowledge that its direction of propagation is  $\mathbf{n}_0$ , then the (unnormalized) electron-photon wave packet should be projected along that direction:

$$\sum_{\sigma} [g_{1\sigma} e^{-i\epsilon_1 t} |1\rangle | \mathbf{n}_0, \sigma, f_1(t) \rangle + g_{2\sigma} e^{-i\epsilon_2 t} |2\rangle | \mathbf{n}_0, \sigma, f_2(t) \rangle]. \quad (11)$$

When the two transitions are very close in frequency, i.e.,  $\eta \equiv |\epsilon_1 - \epsilon_2|/\Gamma \ll 1$ , the overlap of the two photon wave packets deviates from unity by  $\mathcal{O}(\eta)$ . After tracing out the envelopes of the photon by use of any complete basis (e.g., monochromatic states), the state of the electron and photon polarization is, with the propagation direction  $\mathbf{n}_0$  understood,

$$|Y\rangle = \sqrt{N} \sum_{\sigma} [g_{1\sigma} |1\rangle |\sigma\rangle + g_{2\sigma} |2\rangle |\sigma\rangle] + \mathcal{O}(\eta), \quad (12)$$

where  $N$  is a normalization constant, given by

$$N^{-1} = \sum_{j=1,2} \sum_{\sigma=\alpha,\beta} |g_{j\sigma}|^2. \quad (13)$$

The order  $\eta$  error recorded here is meant to indicate the magnitude of the *mixed-state* error which, if neglected, results in a pure state. From this pure state, we can find explicitly the necessary conditions for entanglement or SGC. However, the approximation of neglecting  $\eta$  is unnecessary for computing a measure of entanglement of the resultant mixed state.<sup>15</sup>

### A. Entanglement

A measure of entanglement of the bipartite state  $|Y\rangle$  in Eq. (12) is given by the von Neumann entropy of the reduced density matrix of the state<sup>16</sup> for either the subsystem  $E$  of the two low-lying electronic states or the subsystem  $P$  of the photon polarization states. Taking the partial trace of the polarization states of the density matrix  $|Y\rangle\langle Y|$  of the pure state leads to the  $2 \times 2$  reduced density matrix for the electronic states,

$$\rho_E = N \sum_{ij} |i\rangle \left[ \sum_{\sigma} g_{i\sigma} g_{j\sigma}^* \right] \langle j|. \quad (14)$$

Diagonalization of this partial density matrix leads to two eigenvalues,

$$p_{\pm} = \frac{1}{2} \pm \sqrt{\frac{1}{4} - D^2}, \quad (15)$$

where  $D^2$  is the determinant of the reduced density matrix  $\rho_E$ , or

$$D = N |g_{1\alpha} g_{2\beta} - g_{1\beta} g_{2\alpha}|, \quad (16)$$

for the two electronic state and two polarizations,  $\alpha, \beta$ , normal to the propagation direction  $\mathbf{n}_0$ . The entropy of entanglement is given by the entropy,

$$S = -p_+ \log_2 p_+ - p_- \log_2 p_-. \quad (17)$$

As  $D$  ranges from 0 to  $1/2$ , the entropy ranges from 0 to 1 giving a continuous measure of entanglement as the state  $|Y\rangle$

goes from no entanglement to maximum entanglement. To find the axis  $\mathbf{n}_0$  along which the entanglement is maximum, we have to maximize  $D$  as a function of the orientation. For a particular system, this axis can be found in terms of the dipole matrix elements of the two transitions. However, not all systems can have maximally entangled states. We will apply this to specific examples in the following section.

### B. SGC

From the reduced density matrix, we can also find the conditions for SGC. Maximum SGC occurs when the reduced density matrix is a pure state. In terms of the electron-photon coupling constants, the condition is the vanishing of the discriminant  $D$  in Eq. (16). This means that when the SGC effect is maximized, there exists a particular transformation which takes the basis of the electronic states  $\{|1\rangle, |2\rangle\}$  to a basis  $\{|\mathcal{B}\rangle, |\mathcal{D}\rangle\}$  which has the property that  $|\mathcal{B}\rangle$  is always the final state of the  $\Lambda$  system immediately after the spontaneous emission process, and  $|\mathcal{D}\rangle$  is a state disconnected from the excited state by dipolar coupling, i.e., a dark state. This point will be further explored in Sec. III. The extreme values of  $D=0$  and  $1/2$  make it clear that maximum SGC means no entanglement, and conversely that maximal entanglement leads to no SGC. However, partial entanglement can coexist with the potentiality of some SGC for values of  $D$  between the two extremes.

Our theory can be easily extended to systems with more than two ground states. For example, in a system whose ground states are the four states from two electron spins, the SGC may lead to the coherence and entanglement between the two spins, which is the mechanism of a series of proposals of using vacuum fluctuation to establish entanglement between qubits.<sup>17,18</sup>

### C. Two-pathway decay

So far, we have investigated the consequences when the two transitions are close in frequency ( $\eta \ll 1$ ). When this is not the case, the tracing out of the wave packet will generally produce a mixed state in electron spins and photon polarizations. In the limit of large  $\eta$ , i.e.,  $|\epsilon_2 - \epsilon_1| \gg \Gamma$ , the overlap between the two photon wave functions,  $\langle f_1(t) | f_2(t) \rangle \approx 0$ , and the reduced density matrix for the spin and photon polarization would be mixed. In this case, there is neither spin-polarization entanglement nor SGC, but instead the time development can be described as a two-pathway decay process: The excited state can relax to two different states by the emission of photons with distinct frequencies. For  $\eta$  between these two limits, the state in Eq. (11) may lead to an entanglement between the pulse shapes of the photon and the two lower electronic levels on measuring the photon polarization. Furthermore, from the entangled state in Eq. (11), SGC or polarization entanglement may still be recovered (provided of course that the necessary conditions on the  $g$ 's are satisfied) if the quantum information carried by the frequency of the photon is erased<sup>19</sup>. This can be done by chopping part of the photon pulse, and thus subjecting its frequency to (more) uncertainty. In a time-selective

measurement, only photons emitted at a specific time period, say from  $t_0$  to  $t_0+dt$ , are selected. So the projection operator associated with this measurement is  $p_0=|\delta(t-t_0)\rangle\langle\delta(t-t_0)|$ , which represents a  $\delta$  photon pulse passing the detector at  $t=t_0$ . The projected state after this measurement

$$\sum_{\sigma} [g_1\alpha f_1(t_0)|1\rangle + g_2\alpha f_2(t_0)|2\rangle] |\mathbf{n}_0\sigma\rangle \quad (18)$$

is a pure state of the electron and photon polarization, so that entanglement or SGC is restored. By writing the projector in the frequency domain

$$\tilde{P}_0 = \int d\omega \int d\omega' e^{i(\omega-\omega')t_0} |\omega'\rangle\langle\omega|, \quad (19)$$

we see that it can be understood as a broadband detector with definite phase for each frequency channel; thus, it can erase the frequency (which path) information while retaining the phase correlation. We note that a usual broadband detector without phase correlation is not sufficient to restore the pureness of the state. It is also interesting that SGC and entanglement can be controlled by choosing a different detection time  $t_0$ , as seen from Eq. (18).

### III. SYMMETRY CONSIDERATIONS FOR SGC

In this section, we investigate the symmetry relations between the different parts of the Hamiltonian necessary for SGC terms to appear. Our treatment is not restricted to  $\Lambda$  systems, but can be extended to a system with more than two lower levels.

Consider a quantum mechanical system with one higher-energy level  $|e\rangle$  and a set of lower-lying states, described by a Hamiltonian  $H^\circ$ . Taking into account only dipole-type interactions, denote by  $\mathcal{J}_z$  the polarization operator used in the selection rules. The  $z$  axis is defined by the excited state via

$$\mathcal{J}_z|e\rangle = M_e|e\rangle.$$

Note that  $\mathcal{J}_z$  can be either  $J_z$ , where  $\mathbf{J}=\mathbf{L}+\mathbf{S}$  is the total angular momentum operator and  $\mathbf{S}$  is the spin, or  $L_z$ , as determined by the condition

$$[\mathcal{J}_z, H^\circ] = 0.$$

That is to say that there is an axial symmetry in the system associated with  $\mathcal{J}_z$ . Among the lower lying states, the ones of interest are the ones appearing in the final entangled state  $|Y\rangle$  of the whole system. We will refer to these states as ‘‘bright’’, because they are orthogonal to the familiar dark states from quantum optics. There are at most three such states,  $\{\mathcal{B}_j\}$ , within a given degenerate manifold, corresponding to the three different possible projections of the dipole matrix elements along the  $z$  axis, so  $j=1, 0, \bar{1}$ . In general, not all systems will have all three bright states. This concept that the final state involves only a small number of states (three in our case), gives a physical understanding of the electron-photon entangled state.<sup>20</sup>

In order to have SGC, i.e., one or more terms of the type  $\dot{\rho}_{jk}=\Gamma\rho_{ee}$ , with  $j\neq k$  and  $j, k\neq e$ , there has to be a perturba-

tion  $H^B$  that breaks the symmetry associated with  $\mathcal{J}_z$ ; in particular, the following conditions have to be satisfied:

1.  $[H^B, \mathcal{J}_z] \neq 0$ ;
2.  $H^B|e\rangle \propto |e\rangle$ ;
3.  $|\epsilon_{12}| \leq \Gamma$ .

In general, we expect SGC between two eigenstates of the Hamiltonian  $H=H^\circ+H^B$  which have nonzero overlap with the same bright state. The role of the first condition is to make SGC nontrivial; without this condition, it would always be possible to rotate to a different basis and formally acquire an SGC-like term in the equations (e.g., by rotating to the  $x$  basis in the zero-magnetic field case in the heavy-hole trion system discussed below). The second condition ensures that the excited state will not mix under the action of  $H^B$ ; relaxing this condition gives rise to the Hanle effect,<sup>9,12</sup> in which an ensemble of atoms in a magnetic field is illuminated with an  $x$ -polarized pulse and the reradiated light may be polarized along  $y$ . This effect is another example where coherence plays an important role; it has recently been observed in doped GaAs quantum wells, in the heavy-hole trion system with confinement in one dimension.<sup>21</sup> We shall discuss the quantum dot case below. As shown in Sec. II, when the radiative linewidth of the excited state is smaller than the energy differences of the lower states the SGC effect will be averaged out. The third condition provides the valid regime for the occurrence of this phenomenon.

The perturbation  $H^B$  can be realized by a static electric or magnetic field, by the spin-orbit coupling, hyperfine coupling, etc. Note the different origins of  $H^B$  in different systems and that it may or may not be possible to control  $H^B$ . Examples of various systems follow, exhibiting the above conditions and demonstrating the different origins of  $H^B$ .

### IV. EXAMPLES FROM ATOMIC PHYSICS

#### A. SGC in atoms

Consider an atom with Hamiltonian  $H^\circ$ ; excluding relativistic corrections, it can be diagonalized in the  $|N, L, S, M_L, M_S\rangle$  basis. Consider as the system of interest the subspace of  $H^\circ$  formed by  $|N, 1, 1, 1, 1\rangle=|e\rangle$  and the lower-energy states  $|N-1, L, S, M_L, M_S\rangle$ . The various quantum numbers are, of course, restricted by selection rules, and  $\mathcal{J}_z=L_z$ . Here, we will list only the three bright states:

$$|\mathcal{B}_1\rangle = |N-1, 2, 1, 2, 1\rangle,$$

$$|\mathcal{B}_0\rangle = |N-1, 2, 1, 1, 1\rangle,$$

$$|\mathcal{B}_{\bar{1}}\rangle = a|N-1, 2, 1, 0, 1\rangle + b|N-1, 0, 1, 0, 1\rangle.$$

where the coefficients  $a$  and  $b$  can be determined in the following way. In the original  $|NJM_L S\rangle$  basis, the matrix elements for the transitions  $|N-1, 2, 1, 0, 1\rangle \leftrightarrow |N, 1, 1, 1, 1\rangle$  and  $|N-1, 0, 1, 0, 1\rangle \leftrightarrow |N, 1, 1, 1, 1\rangle$  are given by the Wigner-Eckart theorem. By rotating to the  $\{|\mathcal{B}\rangle, |\mathcal{D}\rangle\}$  basis, and requiring the transition  $|\mathcal{D}\rangle \leftrightarrow |N, 1, 1, 1, 1\rangle$  to be forbidden, we find  $a$  and  $b$ . Inclusion of the spin-orbit interaction, which plays the role of  $H^B$ , i.e.,  $H^B=\alpha\mathbf{L}\cdot\mathbf{S}$ , condition (i) is satisfied, the eigenstates of  $H^B$  being  $|NJM_L S\rangle$ . Condition (ii) is also

satisfied, because  $|e\rangle$ , as the state of maximum  $M_L$  and  $M_S$ , does not mix under the spin-orbit coupling. In the new basis, SGC is expected to occur between states with the same value of  $M_J$ , which can also be verified by direct calculation. In this example, the linewidth of  $|e\rangle$  is much smaller than the spin-orbit coupling strength  $\alpha$ . Typical values in atoms are  $\Gamma_e \sim 1 \mu\text{eV}$  and  $\alpha \sim 1 \text{meV}$ , which means that SGC will not be observed in such a system.

### B. Entanglement and SGC of atomic hyperfine states

In this example, the  $\Lambda$  system is formed by the hyperfine states of a single trapped Cd ion in the presence of a magnetic field along the  $z$  axis. In the  $|FM_F\rangle$  basis, the excited state is  $|21\rangle$  and the two lower levels are  $|11\rangle$  and  $|10\rangle$ . The two lower levels have the same principle quantum number  $N$ . The entanglement between the polarization of the photon and the atom has been demonstrated experimentally.<sup>8</sup> To illustrate the methods developed in Sec. II, we will make use of the fact that the two lower levels are states of definite angular momentum and its projection to the  $z$  axis. Then, by the Wigner–Eckart theorem we know that the dipole moment of the transition  $|21\rangle \rightarrow |10\rangle$  has a nonzero component only along  $\mathbf{e}_+ = \mathbf{x} + i\mathbf{y}$  whereas that of  $|21\rangle \rightarrow |11\rangle$  has only a component along  $\mathbf{z}$ . The wave packet of the system is then given by

$$|\Upsilon\rangle = \frac{-\sqrt{2}\sin\vartheta|\vartheta\rangle|11\rangle + e^{-i\varphi}\cos\vartheta|\vartheta\rangle|10\rangle - ie^{-i\varphi}|\varphi\rangle|10\rangle}{\sqrt{2 + \sin^2\vartheta}}, \quad (20)$$

where  $\vartheta$  and  $\varphi$  are the spherical coordinates measured from  $z$  and  $x$  axis, respectively, and  $|\vartheta\rangle$  and  $|\varphi\rangle$  are the polarization basis states, which are linearly polarized parallel and normal to the plane formed by the  $z$  axis and the propagation direction, respectively. Then, from Eq. (20), we read off the  $g$ 's:

$$g_{1\vartheta} \propto -\sqrt{2}\sin\vartheta, \quad (21)$$

$$g_{1\varphi} = 0, \quad (22)$$

$$g_{2\vartheta} \propto e^{-i\varphi}\cos\vartheta, \quad (23)$$

$$g_{2\varphi} \propto ie^{-i\varphi}, \quad (24)$$

where  $|11\rangle \equiv |1\rangle$  and  $|10\rangle \equiv |2\rangle$ . The measure of entanglement by  $D$  is

$$D = \frac{\sqrt{2}\sin\vartheta}{\sqrt{2 + \sin^2\vartheta}}. \quad (25)$$

The maximum possible entanglement occurs at  $\vartheta = \pi/2$ , i.e., whenever the photon propagates perpendicularly to  $z$ . The maximum value of 0.47 is close to being maximally entangled.  $D$  does not depend on  $\varphi$ , as expected since there is azimuthal symmetry about  $z$ .

In terms of SGC and symmetry, it is interesting to notice that the role of the (external or internal) field,  $H^B$ , introduced in Sec. III can be played by the different projections (measurements) because the state before the measurement is an

eigenstate of the operator  $J_z$  (total angular momentum along  $z$ ), but not after the measurement in general. The magnetic field along the  $z$  axis is included in the Hamiltonian  $H^B$ . If the spontaneously emitted photons are measured along the quantization axis, only the ones emitted from the transition  $|21\rangle \rightarrow |10\rangle$  will be detected, since only their polarization allows propagation along  $z$ . On the other hand, a photon detector placed at a finite angle from  $z$  can play the role of  $H^B$ . Suppose a photon is spontaneously emitted along an axis  $n = (\vartheta, \varphi)$ . The density matrix of the state given by Eq. (20) is  $|\Upsilon\rangle\langle\Upsilon|$ . If we are only interested in the dynamics of the ion, and the polarization of the photon is not measured, then the photon polarization has to be traced out. Then the reduced density matrix of the system in the atomic states is

$$\rho_E = \frac{1}{2 + \sin^2\vartheta} \begin{bmatrix} \cos^2\vartheta + 1 & \sqrt{2}e^{-i\varphi}\cos\vartheta\sin\vartheta \\ \sqrt{2}e^{+i\varphi}\cos\vartheta\sin\vartheta & 2\sin^2\vartheta \end{bmatrix}. \quad (26)$$

The off-diagonal elements express coherence between the hyperfine states with dependence on the photon propagation direction. We can check that for  $\vartheta=0$  the probability of the atom being in the  $|11\rangle$  state is zero and there are no off-diagonal elements, and for  $\vartheta=\pi/2$  the off-diagonal elements are also zero, which means there is no SGC, but the state has the maximum possible entanglement. For all the intermediate values of  $\vartheta$ , the hyperfine states and the photon polarization are entangled, and there is also some SGC when the photon is traced out. Maximum SGC occurs when  $D$  is minimized; from Eq. (25) we see that it is zero for  $\vartheta=0$ . This is expected anytime one of the two transitions involves a linearly polarized photon, since the latter cannot propagate along the quantization axis. So, for this orientation, the final state can only be  $|10\rangle$ . For intermediate angles, for instance  $\vartheta=\pi/4$ , there is both entanglement and SGC involving both lower states, when the photon is traced out. Since SGC only occurs for particular photon propagation directions, we could view it as “probabilistic” SGC.

## V. EXAMPLES FROM SOLID-STATE PHYSICS

### A. Heavy-hole trion system in a magnetic field

In the optical control of the electron spin in a doped quantum dot,<sup>4</sup> a static magnetic field is imposed in a fixed direction at an angle  $\psi$  with respect to the propagation of the circularly polarized pulse along the growth direction of the dot, defined as the  $z$  axis. The two eigenstates of the electron spin along the field direction and the intermediate trion (bound state of an exciton with the excess electron) state in the Raman process form a three-level  $\Lambda$  system. The trion state of interest consists of a  $p$ -like heavy hole and a pair of electrons in the singlet state. The  $g$ -factor in the  $xy$  plane of the heavy hole is approximately zero in magnetic fields up to 5 T (Ref. 22), and the two electrons are in a rotationally invariant state. This means that the trion state, although it is spin polarized along  $z$ , will not precess about a perpendicular  $B$  field. Therefore, it can be described by the “good” quantum numbers  $J=3/2$  and its projection along  $z$ ,  $M_J=3/2$ . The lower levels  $|1\rangle, |2\rangle$  are the eigenstates of the spin along the

direction of the  $B$  field and have  $j=1/2$  and  $m_j=1/2, -1/2$ , respectively.

To check if this system will have SGC, we will examine whether the conditions of Sec. III are satisfied. We take  $H^o$  to be the Hamiltonian of the quantum dot, with  $|e\rangle=|\tau\rangle$ , the trion state described above, excited by  $\sigma+$  light;  $\mathcal{J}_z=J_z$ , since the spin-orbit interaction is included in  $H^o$ , and any component of the  $B$  field along  $z$  can also be included.  $H^B$  is the contribution to the Hamiltonian due to the magnetic field along  $x$ . Condition (1) is fulfilled since  $g_x \approx 0$ , and condition (2) is obviously satisfied. The only bright state is the electron spin  $s_z$  eigenstate,  $|z\rangle \equiv |\uparrow\rangle$ . For later use, we also define  $|\bar{z}\rangle \equiv |\downarrow\rangle$ . Therefore, we expect SGC between states  $|1\rangle$  and  $|2\rangle$  for any angle  $\psi$ , and since the linewidth of the trion is large enough compared to the Zeeman splitting, SGC should moreover have a detectable effect. As a matter of fact, it has already been demonstrated experimentally for this system, and, to the best of our knowledge, it is the only direct observation of SGC.<sup>13</sup> For this nonlinear pump-probe experiment, the inclusion of SGC into the equations causes the amplitude and the phase of the probe signal to depend on the Zeeman splitting. More details on how this dependence occurs will be presented in the following section.

Although our discussion has focused on single  $\Lambda$  systems, the experiment was carried out for an ensemble. In general, for an ensemble of equivalent noninteracting atoms, an average over the different  $z$  axes would have to be performed. However, in this quantum-dot solid-state system, there is a common  $z$  axis for all the dots, since they are grown on the same plane ( $xy$ ), and they have a relatively large in-plane cross-section as compared to their height. This is a clear advantage of the quantum-dot ensemble over an ensemble of atoms.

We can also analyze this system using the methods in Sec. II. To find the  $g$ 's, we need the dipole matrix elements. These can be found by writing

$$|1\rangle = \cos\frac{\psi}{2}|\uparrow\rangle + \sin\frac{\psi}{2}|\downarrow\rangle, \quad (27)$$

$$|2\rangle = \sin\frac{\psi}{2}|\uparrow\rangle - \cos\frac{\psi}{2}|\downarrow\rangle. \quad (28)$$

Again, we will make use of the fact that  $|\uparrow\rangle$  and  $|\tau\rangle$  are angular momentum eigenstates along the  $z$  axis, with the familiar selection rules. Only state  $|\uparrow\rangle$  has a nonzero dipole matrix element with  $|\tau\rangle, d_+ \mathbf{e}_+$ , so that the transitions  $|1\rangle \rightarrow |\tau\rangle$  and  $|2\rangle \rightarrow |\tau\rangle$  have dipole matrix elements equal to  $d_+ \cos\frac{\psi}{2} \mathbf{e}_+$  and  $d_+ \sin\frac{\psi}{2} \mathbf{e}_+$ , respectively. Then, for a photon emitted along  $\mathbf{n}_0 = (\vartheta, \varphi)$ , we find the couplings:

$$g_{1\vartheta} = d_+ e^{i\varphi} \cos\vartheta \cos\frac{\psi}{2}, \quad (29)$$

$$g_{1\varphi} = d_+ e^{i\varphi} \cos\frac{\psi}{2}, \quad (30)$$

$$g_{2\vartheta} = d_+ e^{i\varphi} \cos\vartheta \sin\frac{\psi}{2}, \quad (31)$$

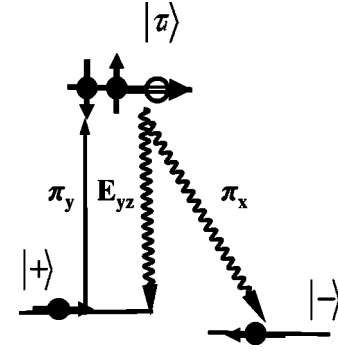


FIG. 1. The energy levels of the  $\Lambda$  system consisting of the two electron spin states (lower levels) and the light-hole trion polarized along the  $+x$  direction. The solid line represents the laser pulse, which propagates along  $z$  and is linearly polarized in the  $y$  direction. The wavy lines denote the spontaneously emitted photons from the transitions  $|\tau\rangle \rightarrow |+\rangle$  and  $|\tau\rangle \rightarrow |-\rangle$ , which are elliptically polarized in the  $yz$  plane and linearly polarized along  $x$ , respectively.

$$g_{2\varphi} = d_+ e^{i\varphi} \sin\frac{\psi}{2}, \quad (32)$$

so that the determinant is always zero, independent of  $\mathbf{n}_0$ . This means that the system in this configuration will never be entangled with the polarization of the photon, which, as we have seen, implies maximum SGC. The final state of the  $\Lambda$  system is always  $|\uparrow\rangle$ , unentangled. Section VI gives an intuitive picture of this concept by the vector representation of (the mean value of) the spin.

### B. Light-hole trion in Voigt configuration

The spin-photon entanglement can be also realized in a quantum-dot system by employing the light-hole trion state. The heavy- and light-hole excitons are split by the breaking of the tetrahedral symmetry of the bulk III-V compound. It might also be possible to make the light-hole states lower in energy than the heavy holes. The magnetic field is pointing along the  $x$  direction, so that the lower levels are the two  $S_x$  eigenstates,  $|+\rangle$  and  $|-\rangle$ . The optical pulses used are such that the light-hole trion polarized along the  $+x$  direction is excited. The excited state is a trion of a singlet pair of electrons and a light hole which is in the  $m_j = \pm 1/2$  component of the  $j = 3/2$  state. The trion can thus be characterized by the state  $|JM_J\rangle = |3/2, \pm 1/2\rangle$ . We choose the  $M_J = 1/2$  state as the excited state of the  $\Lambda$  system and denote it by  $|\tau\rangle$ .

The transitions  $|\tau\rangle \rightarrow |+\rangle$  and  $|\tau\rangle \rightarrow |-\rangle$  involve a photon linearly polarized along  $x$  ( $|X\rangle \equiv |\pi_x\rangle$ ) and one with elliptical polarization ( $-i|Y\rangle + 2|Z\rangle \equiv |E_{yz}\rangle$ ), respectively (see Fig. 1).<sup>23</sup> In particular, after  $|\tau\rangle$  has decayed, the state of the system is from Eq. (12),

$$|Y\rangle = -\frac{1}{\sqrt{6}}[|X\rangle|-\rangle + (2|Z\rangle - i|Y\rangle)|+\rangle], \quad (33)$$

We assume a measurement which determines the propagation direction of the photon  $\mathbf{n}_0 = (\vartheta, \varphi)$ . Then the state becomes:

$$\begin{aligned}
|Y\rangle = & \frac{-1}{\sqrt{2+3\sin^2\vartheta}} [\cos\vartheta\cos\varphi|\vartheta\rangle|-\rangle \\
& - (2\sin\vartheta + i\sin\varphi\cos\vartheta)|\vartheta\rangle|+\rangle \\
& - \sin\varphi|\varphi\rangle|-\rangle - i\cos\varphi|\varphi\rangle|+\rangle]. \quad (34)
\end{aligned}$$

Following the same procedure as in the trapped ion example, we find that the condition for maximum entanglement is  $\vartheta = 0$ ; the value of  $D$  is then 0.5, maximal entanglement. SGC will only occur when  $D$  in Eq. (16) is less than 0.5 and it will be maximum for propagation along  $x$ , which means that the electron will be in the state  $|+\rangle$ . For all other values of  $\vartheta$ , there will be both entanglement and SGC between the two energy eigenstates when the photon is traced out. The phenomena following the spontaneous radiative decay of this system are indeed very similar to the trapped ion case. In the solid-state system, there is no need to isolate a single dot in order to observe SGC since all dots are oriented in the same direction.

For quantum information processing, entanglement between photon polarization and spin has to be established in a quantum dot. So isolating and addressing a single dot is required. Experimentally, this requirement is arguably feasible.<sup>24</sup> The system should be initialized at state  $|+\rangle$  (or  $|-\rangle$ ) and subsequently excited by  $y$ - (or  $x$ -) polarized light, so that only state  $|\tau_j\rangle$  gets excited. Other trion states, involving electrons in the triplet state and/or heavy holes, have an energy separation from  $|\tau_j\rangle$  large enough compared to the pulse bandwidth and so they can be safely ignored. Above, we found that the state will be maximally entangled when the spontaneously emitted photon propagates along  $z$ . When the optical axis is along  $z$ , the spontaneously emitted photon may be distinguished from the laser photons by optical gating. As an alternative to the optical gating, to minimize scattered light the detector may be placed along  $y$ , i.e., at  $(\vartheta, \varphi) = (\pi/2, \pi/2)$ . The value of  $D$  is then 0.2, so that the entanglement will be significantly less than that along the optical axis, but should be measurable. The observation of the emitted photon and the measurement of its polarization can be made as in Ref. 8. By use of the pump-probe technique, the state of the spin will also be measured to show the correlation with the polarization of the photon.

To overcome the probabilistic nature of the entanglement (as projection is needed) and to improve the quantum efficiency degraded by the scattering problem, cavities and waveguides may be employed to enhance and select desired photon emission processes.<sup>7,25</sup>

## VI. PUMP-PROBE EXPERIMENT FOR SGC DETECTION IN A QUANTUM DOT

In this section, we provide a theoretical analysis for the pump-probe experiment which explicitly demonstrated SGC.<sup>13</sup> The  $\Lambda$  system is the heavy-hole trion system introduced above. We present a treatment based on the idea that SGC may be viewed as a decay to one bright state which is a superposition of the eigenstates. The vector character of the mean value of the spin, which also helps develop intuition for the SGC effect, is employed and in fact it anticipates

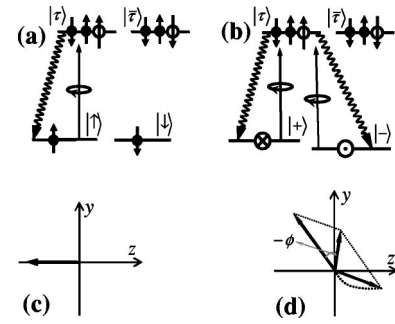


FIG. 2. (a) and (b) are the energy diagrams and possible electron-trion transitions caused by  $\sigma+$ -polarized photons with the electron spin quantized in  $z$  and  $x$  directions, respectively. (c) The Raman coherence generated by the pump pulse, and (d) Schematic depiction of interference between the Raman coherence and the spin coherence generated by spontaneous emission, under a magnetic field applied along the  $x$  direction.

some of the theoretical results of the pump-probe measurements calculated by perturbative solution of the density matrix in the remainder of this section.

### A. Geometrical picture of SGC

As shown by Bloch<sup>26</sup> and Feynman *et al.*,<sup>27</sup> an ensemble of two-level systems can be described by a rotating vector. This picture provides an intuitive understanding of the spin coherence generated by the optical excitation and spontaneous decay of the trion states. For simplicity, we will assume the short-pulse limit in this section.

Regardless of the presence or absence of the quantization direction, there is freedom in the choice of the quantization direction, and it is convenient in this case to choose the spin eigenstates quantized in the growth ( $z$ ) direction,  $|\uparrow\rangle$  and  $|\downarrow\rangle$ . The two trion states  $|\tau\rangle$  and  $|\bar{\tau}\rangle$  have  $J=3/2$  and  $z$ -component  $M=+3/2$  and  $M=-3/2$ , respectively. The selection rules are such that a photon with helicity  $\pm 1$  ( $\sigma\pm$  circular polarization) excites the electron  $|\uparrow\rangle$  or  $|\downarrow\rangle$  to the trion states  $|\tau\rangle$  or  $|\bar{\tau}\rangle$ , respectively. We will consider a  $\sigma+$  polarized pump, which excites spin-up electrons to the trion state  $|\tau\rangle$ , leaving the electron spin polarized in the  $-z$  direction. Due to the selection rules, the trion state can only relax back to the spin-up state by emitting a  $\sigma+$  polarized photon, and after recombination, the electron remains unpolarized.

Now let us consider a strong magnetic field, applied at  $\psi = \pi/2$  with respect to the optical axis,  $\mathbf{B} = B\mathbf{e}_x$ . In this so-called Voigt configuration, the Zeeman states  $|\pm\rangle \equiv (|\uparrow\rangle \pm |\downarrow\rangle)/\sqrt{2}$  are quantized in the  $x$  direction and are energy eigenstates with energies  $\pm\omega_L$ , respectively, while the trion states can still be assumed quantized in the  $z$  direction [see Fig. 2(b)]. Note that the low-lying states  $|1\rangle, |2\rangle$  in foregoing sections are now denoted by the spin states,  $|+\rangle, |-\rangle$ . In the short-pulse limit, the pulse spectrum is much broader than the spin splitting or, equivalently, the pulse duration is much shorter than the spin precession period, so the excitation process is virtually unaffected by the magnetic field: the  $\sigma+$  polarized pump excites the  $|\uparrow\rangle$  electron to the trion state  $|\tau\rangle$ , leaving the electrons spin polarized in the  $-z$  direction, as

in the zero-field case [see Fig. 2(c)]. The pulse generates coherence between the two eigenstates  $|+\rangle$  and  $|-\rangle$ , which is the conventional Raman coherence<sup>28</sup> generated by a pulse with a spectrum broad enough to cover both the near-degenerate transitions. The spin precesses in the magnetic field normal to the plane of precession with frequency  $\omega_L/\pi$ . In other words, the state oscillates between the spin-up and -down states. The Raman coherence can be determined by the excitation-induced change of the population in the spin state  $|\uparrow\rangle$ ,

$$\rho_{\uparrow\uparrow}^R(t) = -\frac{\rho_{\tau\tau}}{2} [1 + \cos(2\omega_L t) e^{-\gamma_2 t}], \quad (35)$$

where  $\rho_{\tau\tau}$  is the population of the trion state immediately after the excitation pulse, and  $\gamma_2$  is the damping rate of the spin polarization (due to spin dephasing and inhomogeneous broadening).

On the other hand, when the system is in the trion state  $|\tau\rangle$ , the trion will relax by emitting a  $\sigma+$ -polarized photon, leaving an electron spin polarized in the  $+z$  direction, i.e., generating coherence between the two spin eigenstates (SGC). The trion decay can be treated as a stochastic quantum jump process with the jump rate  $2\Gamma$ . After the quantum jump, the evolution of the system can be described by a spin vector rotating under the transverse magnetic field. Thus, the spin polarization generated by the spontaneous emission during  $[t', t' + dt']$  can be determined by

$$d\rho_{\uparrow\uparrow}^{\text{SGC}}(t, t') = \frac{\rho_{\tau\tau} e^{-2\Gamma t'} 2\Gamma dt'}{2} [1 + \cos(2\omega_L(t-t')) e^{-\gamma_2(t-t')}]. \quad (36)$$

The precessing spin vector is deformed by the accumulation of increments through the optical decay into a spiral curve [see Fig. 2(d)]. The accumulated spin polarization due to the spontaneous emission is

$$\begin{aligned} \rho_{\uparrow\uparrow}^{\text{SGC}}(t) &= \int_0^t d\rho_{\uparrow\uparrow}^{\text{SGC}}(t, t') \\ &= \frac{\rho_{\tau\tau}}{2} \Re \left[ 1 - e^{-2\Gamma t} + \frac{2\Gamma}{2\Gamma - \gamma_2 - i2\omega_L} \right. \\ &\quad \left. \times (e^{-i2\omega_L t - \gamma_2 t} - e^{-2\Gamma t}) \right]. \end{aligned} \quad (37)$$

For an initially unpolarized system, the total spin polarization in the  $z$  direction after the action of the pump and the recombination process is given by

$$\begin{aligned} \rho_{\uparrow\uparrow}^{(2)} &= [\rho_{\uparrow\uparrow}^R + \rho_{\uparrow\uparrow}^{\text{SGC}}] \\ &= -\frac{\rho_{\tau\tau}}{2} [(1 + a_\Gamma) e^{-2\Gamma t} + a_0 \cos(2\omega_L t - \phi) e^{-\gamma_2 t}], \end{aligned} \quad (38)$$

where

$$a_\Gamma \equiv \frac{2\Gamma(2\Gamma - \gamma_2)}{(2\Gamma - \gamma_2)^2 + 4\omega_L^2}, \quad (39)$$

$$a_0 \equiv \sqrt{\frac{\gamma_2^2 + 4\omega_L^2}{(2\Gamma - \gamma_2)^2 + 4\omega_L^2}}, \quad (40)$$

$$\phi \equiv -\arctan \frac{2\Gamma - \gamma_2}{2\omega_L} - \arctan \frac{\gamma_2}{2\omega_L}. \quad (41)$$

As shown in Fig. 2(d), SGC induces a phase shift of the spin coherence as compared to the Raman coherence. Note also the different amplitudes of the Bloch vectors in the case with and without SGC. We can see that if the recombination is much faster than the spin precession under the magnetic field, i.e.,  $\Gamma \gg \omega_L$ , SGC actually cancels the Raman coherence. This is not surprising since such a limit simply corresponds to the zero-field case. In the strong field limit where  $\omega_L \gg \Gamma$ , the spin precession will average SGC to zero, which corresponds to the two-pathway decay discussed in Sec. II. From Eq. (36), it can be seen that at any specific time the trion relaxes to state  $|\uparrow\rangle$ , so, as shown in Sec. II, a time-selective measurement can recover the SGC from the incoherent two-pathway decay. Without such a projection, as the spin coherence generated at a different time has a different phaseshift, the time averaging [see Eq. (37)] leads to the vanishing of the SGC.

In a pump-probe experiment, what is measured is the differential transmission signal (DTS), i.e., the difference between the probe transmission with and without the pump pulse. In the same-circular polarization (SCP) pump-probe configuration, the probe measures the change in the population difference created by the pump,  $\rho_{\tau\tau} - \rho_{\uparrow\uparrow}^{(2)}$ . Hence, the DTS is given by

$$\Delta T^{\text{SCP}} \propto (3 + a_\Gamma) e^{-2\Gamma t_d} + a_0 \cos(2\omega_L t_d - \phi), \quad (42)$$

where  $t_d$  is the delay time between the pump and probe pulses. The DTS reveals the spin beatings and the SGC effect manifests itself in the dependence of the beat amplitude and phase shift on the strength of the magnetic field.

The pump-probe experiment can also be done in the opposite circular polarization (OCP) configuration. The probe measures the change of population of the spin-down state  $|\downarrow\rangle$ . The DTS in this case is proportional to  $-\rho_{\downarrow\downarrow}^{(2)} = \rho_{\uparrow\uparrow}^{(2)} + \rho_{\tau\tau}$  i.e.,

$$\Delta T^{\text{OCP}} \propto (1 - a_\Gamma) e^{-2\Gamma t_d} - a_0 \cos(2\omega_L t_d - \phi). \quad (43)$$

The spin beat has the opposite sign to the SCP case.

Similar analysis shows that if either the pump or the probe pulse is linearly polarized, there will be no spin beat in the DTS.

## B. Perturbative solution of the probe signal

The optical field of the pump and probe pulses can be written as

$$\begin{aligned} \mathbf{E}(t) &= (\mathbf{e}_+ E_{1+} + \mathbf{e}_- E_{1-}) \chi_1(t) e^{-i\Omega_1 t} \\ &\quad + (\mathbf{e}_+ E_{2+} + \mathbf{e}_- E_{2-}) \chi_2(t - t_d) e^{-i\Omega_2(t-t_d)}, \end{aligned} \quad (44)$$

where the subscripts 1 and 2 denote the pump and probe pulses, respectively, and  $\mathbf{e}_\pm$  are the unit vectors of the  $\sigma_\pm$  polarizations. The dipole operator is

$$\hat{\mathbf{d}} = d(\mathbf{e}_+|\tau\rangle\langle\bar{\tau}| \pm \mathbf{e}_-|\bar{\tau}\rangle\langle\pm|) + \text{h.c.}$$

Thus, in the rotating wave approximation, the Hamiltonian in the basis  $\{|-\rangle, |+\rangle, |\tau\rangle, |\bar{\tau}\rangle\}$  can be written in matrix form as

$$H = \begin{bmatrix} -\omega_L & 0 & -d^*E_+(t) & -d^*E_-(t) \\ 0 & \omega_L & -d^*E_+(t) & +d^*E_-(t) \\ -dE_+(t) & -dE_-(t) & \epsilon_g & 0 \\ -dE_-(t) & +dE_-(t) & 0 & \epsilon_g \end{bmatrix}, \quad (45)$$

where  $\epsilon_g$  is the energy of the trion states, and  $\gamma_1, \gamma_2$ , and  $2\Gamma$  denoting the spin-flip rate, the spin-depolarizing rate, and the trion decay rate, respectively. The explicit equations for each element of the density matrix are

$$\dot{\rho}_{\tau,+} = i[\rho, H]_{\tau,+} - \Gamma\rho_{\tau,+}, \quad (46)$$

$$\dot{\rho}_{\tau,-} = i[\rho, H]_{\tau,-} - \Gamma\rho_{\tau,-}, \quad (47)$$

$$\dot{\rho}_{+,+} = i[\rho, H]_{+,+} - \gamma_1\rho_{+,+} + \Gamma(\rho_{\tau\tau} + \rho_{\bar{\tau}\bar{\tau}}), \quad (48)$$

$$\dot{\rho}_{-,-} = i[\rho, H]_{-,-} + \gamma_1\rho_{+,+} + \Gamma(\rho_{\tau\tau} + \rho_{\bar{\tau}\bar{\tau}}), \quad (49)$$

$$\dot{\rho}_{+,-} = i[\rho, H]_{+,-} - \gamma_2\rho_{+,-} + \Gamma_c(\rho_{\tau\tau} - \rho_{\bar{\tau}\bar{\tau}}), \quad (50)$$

$$\dot{\rho}_{\tau\tau} = i[\rho, H]_{\tau\tau} - 2\Gamma\rho_{\tau\tau}, \quad (51)$$

$$\dot{\rho}_{\bar{\tau}\bar{\tau}} = i[\rho, H]_{\bar{\tau}\bar{\tau}} - 2\Gamma\rho_{\bar{\tau}\bar{\tau}}, \quad (52)$$

$$\dot{\rho}_{\bar{\tau}\tau} = i[\rho, H]_{\bar{\tau}\tau} - 2\Gamma\rho_{\bar{\tau}\tau}. \quad (53)$$

The Markov-Born approximation for the system photon has been employed. The term representing the spontaneously

generated spin coherence due to the trion recombination is indicated by the suffix  $c$ ;  $\Gamma_c$  should be equal to  $\Gamma$ . However, we singled out the SGC term so that  $\Gamma_c$  can be artificially set to zero for a theoretical comparison between the results with and without the SGC effect.

In the pump-probe experiment, the DTS corresponds to the third-order optical response. The absorption of the probe pulse is proportional to the work  $W$  done by the probe pulse, and the DTS is<sup>29</sup>

$$\begin{aligned} \Delta T \propto -W^{(3)} &= -2\Re \int \dot{\mathbf{P}}^{(3)}(t) \cdot \mathbf{E}_2^*(t - t_d) \\ &\approx -2\Omega_2\tilde{\gamma} \int \tilde{\mathbf{P}}^{(3)}(\omega + \Omega_2) \cdot \tilde{\mathbf{E}}_2^*(\omega + \Omega_2) \frac{d\omega}{2\pi}. \end{aligned} \quad (54)$$

The third-order optical polarization of the system can be calculated directly by expanding the density matrix according to the order of the optical perturbation

$$\mathbf{P}^{(3)} = \mathbf{e}_+d[\rho_{\tau,-}^{(3)} + \rho_{\tau,+}^{(3)}] + \mathbf{e}_-d[\rho_{\bar{\tau},-}^{(3)} - \rho_{\bar{\tau},+}^{(3)}], \quad (55)$$

Thus, given the  $\sigma+$ -polarized pump pulse, the third-order polarization in the SCP and OCP cases can be respectively calculated as<sup>29</sup>

$$\mathbf{P}_{\text{SCP}}^{(3)}(t) = \mathbf{e}_+d[\rho_{\tau,-}^{(3)}(t) + \rho_{\tau,+}^{(3)}(t)], \quad (56)$$

$$\mathbf{P}_{\text{OCP}}^{(3)}(t) = \mathbf{e}_-d[\rho_{\bar{\tau},-}^{(3)}(t) - \rho_{\bar{\tau},+}^{(3)}(t)]. \quad (57)$$

### C. Analytical results

The density matrix can be calculated straightforwardly order by order with respect to the pulse. Taking the initial state of the system to be the equilibrium state  $\rho^{(0)} = \rho_+^{(0)}|+\rangle\langle+| + \rho_-^{(0)}|-\rangle\langle-|$ . The result for the second-order spin coherence due to the pump pulse  $\mathbf{E}_1(t)$  is:

$$\begin{aligned} \tilde{\rho}_{+,-}^{(2)}(\omega) &= +X_1 \frac{\rho_-^{(0)}}{\omega - 2\omega_L + i\gamma_2} \int_{-\infty}^{+\infty} \frac{\chi_1^*(\omega' - \omega)\chi_1(\omega') d\omega'}{\omega' - \Delta_1 - \omega_L + i\Gamma} \frac{d\omega'}{2\pi} - X_1 \frac{\rho_+^{(0)}}{\omega - 2\omega_L + i\gamma_2} \int_{-\infty}^{+\infty} \frac{\chi_1(\omega' + \omega)\chi_1^*(\omega') d\omega'}{\omega' - \Delta_1 + \omega_L - i\Gamma} \frac{d\omega'}{2\pi} \\ &+ X_1 \frac{i\Gamma_c\rho_{\pm}^{(0)}}{(\omega - 2\omega_L + i\gamma_2)(\omega + i2\Gamma)} \int_{-\infty}^{+\infty} \frac{\chi_1(\omega' + \omega)\chi_1^*(\omega') d\omega'}{\omega' - \Delta_1 \pm \omega_L - i\Gamma} \frac{d\omega'}{2\pi} - X_1 \frac{i\Gamma_c\rho_{\pm}^{(0)}}{(\omega - 2\omega_L + i\gamma_2)(\omega + i2\Gamma)} \int_{-\infty}^{+\infty} \frac{\chi_1^*(\omega' - \omega)\chi_1(\omega') d\omega'}{\omega' - \Delta_1 \pm \omega_L + i\Gamma} \frac{d\omega'}{2\pi}, \end{aligned} \quad (58)$$

where  $\Delta_1 \equiv \epsilon_g - \Omega_1$  is the detuning, and  $X_1 \equiv |dE_{1,+}|^2 - |dE_{1,-}|^2$  is the circular degree of the pulse polarization. In the equation above, the first two terms correspond to the Raman coherence generated by the pump excitation<sup>28</sup>, and the last two terms represent the spontaneously generated coherence. Obviously, for a linearly polarized pump,  $X_1=0$ , no spin coherence is generated either by excitation or by recombination, so there will be no spin beats in DTS.

In the short-pulse limit, the spin coherence after the pump and recombination can be approximately expressed as

$$\rho_{+,-}^{(2)}(t) \approx X_1 |\chi_1(\Delta_1)|^2 \left( \frac{\Gamma_c}{2\Gamma - \gamma_2 - 2i\omega_L} - \frac{1}{2} \right) e^{-i(2\omega_L - i\gamma_2)(t-t_1)}. \quad (59)$$

This formula can be directly compared to the result obtained by the intuitive picture in Sec. VI A. The physical meaning

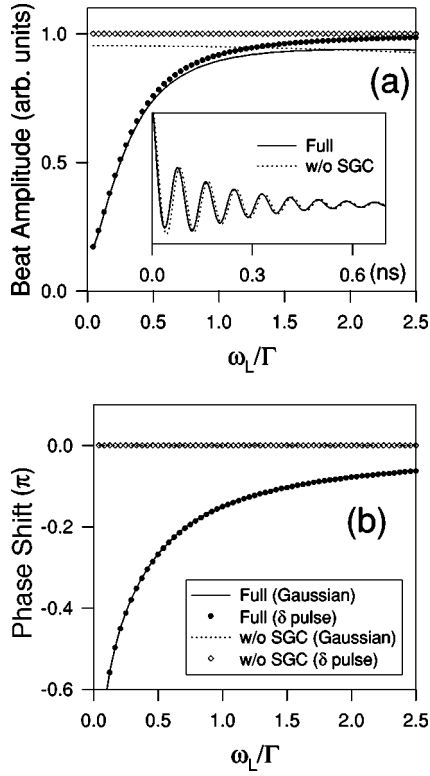


FIG. 3. (a) The amplitude and (b) the phase shift of the spin beat (shown in the insert) as functions of the Zeeman splitting in units of the trion state width,  $\Gamma$ . The filled circle and solid lines include the SGC effect, calculated with and without the short-pulse approximation, respectively. The diamond and dotted lines are the results without the SGC effect, calculated with and without the short-pulse approximation, respectively.

of the two terms in Eq. (59) is transparent: The first term is SGC, whose amplitude and phase shift depend on the ratio of the recombination rate to the Zeeman splitting, and the second term is just the optically pumped Raman coherence which in the short pulse limit is independent of the Zeeman splitting.

Having obtained the second-order results, we can readily derive the third-order density matrix and, in turn, the DTS can be calculated by use of Eq. (54). In general, the DTS can be expressed as

$$\Delta T \propto A \cos(2\omega_L t_d - \phi) e^{-\gamma_2 t_d} + B e^{-2\Gamma t_d} + C e^{-\gamma_1 t_d}, \quad (60)$$

and the spin coherence amplitude  $A$  and phase shift  $\phi$ , the Pauli blocking amplitude  $B$ , and the spin nonequilibrium population  $C$  can all be numerically calculated and, in the short-pulse limit, can also be analytically derived as

$$A \approx |\chi_1(\Delta_1)|^2 |\chi_2(\Delta_2)|^2 X_1 X_2 \sqrt{\frac{\gamma_2^2 + 4\omega_L^2}{(2\Gamma_c - \gamma_2)^2 + 4\omega_L^2}}, \quad (61)$$

$$\phi \approx -\arctan\left(\frac{2\Gamma_c - \gamma_2}{2\omega_L}\right) - \arctan\left(\frac{\gamma_2}{2\omega_L}\right), \quad (62)$$

$$B \approx |\chi_1(\Delta_1)|^2 |\chi_2(\Delta_2)|^2 \left[ I_1 I_2 + 2I_{1+} I_{2+} + 2I_{1-} I_{2-} + X_1 X_2 \frac{2\Gamma_c(2\Gamma - \gamma_2)}{(2\Gamma - \gamma_2)^2 + 4\omega_L^2} \right], \quad (63)$$

$$C \approx 0, \quad (64)$$

where  $\Delta_2 \equiv \epsilon_g - \Omega_2$  is the detuning,  $I_{j\pm} \equiv |dE_{j\pm}|^2$ ,  $I_j \equiv I_{j+} + I_{j-}$ , and  $X_j \equiv I_{j+} - I_{j-}$  ( $j=1$  or  $2$ ). Thus, the short-pulse approximation yields expressions identical to the ones obtained from the intuitive picture in Sect. VI A. Several conclusions can be immediately drawn from the short-pulse approximation: (1) The SCP and OCP signals reveal beats with the same amplitude and opposite signs; (2) no spin beat can be observed when either of the pulses is linearly polarized ( $X_1 = 0$  or  $X_2 = 0$ ); and (3) due to the SGC effect, the beat amplitude increases with increasing Zeeman splitting until it saturates at the value it would have in the absence of the SGC effect; the phase shift increases from  $-\pi/2$ , saturating at 0. The SGC effect is negligible when the Zeeman splitting is large compared to the trion decay rate  $\Gamma$  because the rapid oscillation averages the effect of SGC to zero.

#### D. Numerical results

In the numerical simulations, we take the pump and the probe envelopes to be Gaussian  $\chi_1(t) = \exp(-\eta_1^2 t^2/2)$  and  $\chi_2(t-t_d) = \exp(-\eta_2^2 (t-t_d)^2/2)$ , and we assume that they have no temporal overlap, i.e., the delay time  $t_d$  is much larger than the pulse duration  $\eta_j^{-1}$  ( $j=1,2$ ), and the pulse bandwidth  $\eta_j$  is greater than the relaxation rates  $\gamma_1$ ,  $\gamma_2$ , and  $\Gamma$ . All these assumptions are well satisfied in the experiment.<sup>13</sup> Taken from the experiment,<sup>13</sup> the relaxation rates used are  $\gamma_1 = 0$ ,  $\gamma_2 = 3 \mu\text{eV}$ , and  $\Gamma = \Gamma_c = 12 \mu\text{eV}$ , and  $\eta_1 = \eta_2 = 0.5 \text{ meV}$ .

To minimize the effect of the background noise,<sup>13</sup> the measured data of DTS are presented as the difference between the SCP and OCP. We follow the same practice in presenting the theoretical results in Fig. 3. In comparison with the results without the SGC effect (dashed line), the full theoretical results show the phase shift of the spin beat in the DTS.

In Fig. 3, the amplitude and the phase shift are plotted against the Zeeman splitting  $2\omega_L$ , which is proportional to the magnetic field. The SGC effect is evident through the field dependence of the amplitude and phase shift of the spin beat. When the SGC effect is artificially switched off (by setting  $\Gamma_c = 0$ ), the beat is independent of the magnetic field strength as long as the pulse spectrum is much broader than the Zeeman splitting. In the weak magnetic field limit, the spin coherence is strongly suppressed due to the destructive interference between the conventional Raman coherence and SGC; the phase shift then is about  $-\pi/2$ . In the strong magnetic field limit, as SGC is averaged to zero due to the rapid Larmor precession, the beat features approach those calculated without SGC. The theoretical predictions of the SGC effect on the pump-probe signals are in good agreement with the experimental results.<sup>13</sup>

## VII. CONCLUSIONS

In this work, we have developed a theory to unite the different effects emerging from the spontaneous emission of a photon from a  $\Lambda$  system. We have taken the viewpoint that spontaneous emission is a unitary process when a sufficiently large quantum system is defined so as to be considered closed. Then the final state of the whole system, which is a pure state, can be projected in different ways. These projections can be thought of as measurements on one of the constituent parts and give rise to different phenomena: entanglement, spontaneously generated coherence, and two-pathway decay. We have also presented a set of conditions on the symmetry of a system which determine if there is SGC. Examples of specific atomic and solid-state systems have been

employed to illustrate our theory. We have sketched the theory underlying the experiment in which SGC was observed<sup>13</sup> and we have proposed an experiment on the same system to exhibit the entanglement between the electron spin and the polarization of the spontaneously emitted photon in a quantum dot in parallel to the atom case.<sup>8</sup>

## ACKNOWLEDGMENTS

This work was supported by ARDA/ARO under grant W911NF-04-1-0235 and a Graduate Fellowship DAAD19-02-10183. One of the authors (S.E.E.) also acknowledges a graduate fellowship from the Alexander S. Onassis Public Benefit Foundation.

- 
- <sup>1</sup>S. E. Harris, J. E. Field, and A. Imamoglu, *Phys. Rev. Lett.* **64**, 1107 (1990).
- <sup>2</sup>S. E. Harris, *Phys. Rev. Lett.* **62**, 1033 (1989).
- <sup>3</sup>A. Imamoglu, D. D. Awschalom, G. Burkard, D. P. DiVincenzo, D. Loss, M. Sherwin, and A. Small, *Phys. Rev. Lett.* **83**, 4204 (1999).
- <sup>4</sup>A. Shabaev, A. L. Efros, D. Gammon, and I. A. Merkulov, *Phys. Rev. B* **68**, 201305(R) (2003); P. Chen, C. Piermarocchi, L. J. Sham, D. Gammon, and D. G. Steel, *ibid.* **69**, 075320 (2004).
- <sup>5</sup>C. Monroe, D. M. Meekhof, B. E. King, W. M. Itano, and D. J. Wineland, *Phys. Rev. Lett.* **75**, 4714 (1995).
- <sup>6</sup>G. K. Brennen, C. M. Caves, P. S. Jessen, and I. H. Deutsch, *Phys. Rev. Lett.* **82**, 1060 (1999).
- <sup>7</sup>R. B. Liu, W. Yao, and L. J. Sham, cond-mat/0408148 (unpublished).
- <sup>8</sup>B. B. Blinov, D. L. Moehring, L.-M. Duan, and C. Monroe, *Nature (London)* **428**, 153 (2004).
- <sup>9</sup>C. Cohen-Tannoudji, J. Dupont-Roc, and G. Grynberg, *Atom-Photon Interactions* (Wiley, New York, 1992).
- <sup>10</sup>D. A. Cardimona and C. R. Stroud, Jr., *Phys. Rev. A* **27**, 2456 (1983).
- <sup>11</sup>J. Javanainen, *Europhys. Lett.* **17**, 407 (1992).
- <sup>12</sup>M. O. Scully and M. S. Zubairy, *Quantum Optics* (Cambridge University Press, Cambridge, UK, 1997).
- <sup>13</sup>M. V. G. Dutt *et al.* (unpublished).
- <sup>14</sup>V. Weisskopf and E. Wigner, *Z. Phys.* **63**, 54 (1930).
- <sup>15</sup>C. H. Bennett, D. P. DiVincenzo, J. A. Smolin, and W. K. Wootters, *Phys. Rev. A* **54**, 3824 (1996).
- <sup>16</sup>W. K. Wootters, *Phys. Rev. Lett.* **80**, 2245 (1998).
- <sup>17</sup>M. B. Plenio, S. F. Huelga, A. Beige, and P. L. Knight, *Phys. Rev. A* **59**, 2468 (1999).
- <sup>18</sup>X.-L. Feng, Z.-M. Zhang, X.-D. Li, S.-Q. Gong, and Z.-Z. Xu, *Phys. Rev. Lett.* **90**, 217902 (2003).
- <sup>19</sup>Y.-H. Kim, R. Yu, S. P. Kulik, Y. Shih, and M. O. Scully, *Phys. Rev. Lett.* **84**, 1 (2000).
- <sup>20</sup>K. W. Chan, C. K. Law, and J. H. Eberly, *Phys. Rev. Lett.* **88**, 100402 (2002).
- <sup>21</sup>R. I. Dzhdzhoiev, V. L. Korenev, B. P. Zakharchenya, D. Gammon, A. S. Bracker, J. G. Tischler, and D. S. Katzer, *Phys. Rev. B* **66**, 153409 (2002).
- <sup>22</sup>J. G. Tischler, A. S. Bracker, D. Gammon, and D. Park, *Phys. Rev. B* **66**, 081310(R) (2002).
- <sup>23</sup>A. A. Kiselev, K. W. Kim, and E. Yablonovitch, *Phys. Rev. B* **64**, 125303 (2001).
- <sup>24</sup>N. H. Bonadeo, J. Erland, D. Gammon, D. Park, D. S. Katzer, and D. G. Steel, *Science* **282**, 1473 (1998).
- <sup>25</sup>W. Yao, R. B. Liu, and L. J. Sham, quant-ph/0407060 (unpublished).
- <sup>26</sup>F. Bloch, *Phys. Rev.* **70**, 460 (1946).
- <sup>27</sup>R. P. Feynman, F. L. Vernon, Jr., and R. W. Hellwart, *J. Appl. Phys.* **28**, 49 (1957).
- <sup>28</sup>R. Leonhardt, W. Holzzapfel, W. Zinth, and W. Kaiser, *Chem. Phys. Lett.* **133**, 373 (1987).
- <sup>29</sup>N. Bloembergen, *Nonlinear Optics* (World Scientific, Singapore, 1996).